Comparative Study on Adsorptive Removal of Thiophenic Sulfurs over Y and USY Zeolites

ARTICLE *in* INDUSTRIAL & ENGINEERING CHEMISTRY RESEARCH · SEPTEMBER 2008

Impact Factor: 2.59 · DOI: 10.1021/ie701785s

3 AUTHORS:

Sakdinun Nuntang
Mae Jo University
4 PUBLICATIONS **49** CITATIONS
SEE PROFILE

Pattarapan Prasassarakich
Chulalongkorn University
94 PUBLICATIONS **1,063** CITATIONS
SEE PROFILE

Chawalit Ngamcharussrivichai
Chulalongkorn University
35 PUBLICATIONS **701** CITATIONS
SEE PROFILE

Comparative Study on Adsorptive Removal of Thiophenic Sulfurs over Y and USY Zeolites

Sakdinun Nuntang, Pattarapan Prasassarakich, and Chawalit Ngamcharussrivichai*

Fuels Research Center, Department of Chemical Technology, Faculty of Science, Chulalongkorn University, Bangkok 10330, Thailand

Removal of organic sulfur compounds by using an adsorption process was carried out at ambient temperature and pressure. FAU zeolites, including NaY, HUSY cation-exchanged with metal ions such as Cu, Ni, Zn, and La, have been applied as adsorbents in the desulfurization of model and real transportation fuels. The results showed that the type of metal ion-exchanged, amount of metal ion-exchanged, and structure of zeolite have important roles in the removal of each organic sulfur. LaNaY, LaHUSY, and CuNaY possessed highest adsorption capacity toward thiophene (TH), benzothiophene (BT), and dibenzothiophene (DBT), respectively. Among the tested adsorbents, LaHUSY exhibited highest adsorption selectivity to BT and DBT in the presence of naphthalene. The comparative study indicated that La^{3+} is capable of strongly adsorbing the aromatic sulfur compounds via both direct interaction at sulfur atom and via π-electronic interaction. Adsorptive desulfurization of real diesel over LaHUSY reduced the sulfur level from 229 to less than 50 ppm, and the adsorption selectivity to 4-methyldibenzothiophene (4-MDBT) was highest.

Introduction

Gasoline and diesel are the main transportation fuels in the world. On the basis of the current situation, they are still produced from petroleum and inevitably contain a significant amount of organic sulfurs, up to 300 ppm in gasoline and 500 ppm in diesel. Combustion of these fuels in internal combustion engines emits SO_x as a major air pollutant. Moreover, it can poison the catalyst designed for exhaust gas treatment even at low concentration. The removal of organic sulfurs from transportation fuels is becoming a more and more important issue due to stringent environmental legislation. Following the new regulations announced by the U.S. Environmental Protection Agency (EPA) and European Union (EU),[1−4] Thailand also states the regulation of the sulfur level in gasoline and diesel fuel limit to less than 50 ppm by 2010.

Hydrodesulfurization (HDS) using $NiMo/Al_2O_3$ and $CoMo/Al_2O_3$ catalysts is the conventional process being employed in the refineries worldwide to remove sulfur compounds from the transportation fuels. Recently, some new catalyst formulations have been developed to improve the efficiency of HDS processes.[5−7] However, the HDS process is not economic to produce ultraclean transportation fuels, since the removal of refractory sulfur compounds, including thiophene (TH), benzothiophene (BT), dibenzothiophene (DBT), and their derivatives, requires high temperatures and high H_2 pressure. Selective adsorption of the sulfur compounds from particular petroleum fractions has been considered as an effective way to reduce the sulfur level without treating the whole fuel under such severe conditions.[8,9]

Among the several types of adsorbents reported in the literature, zeolites have been found to be promising materials for adsorptive desulfurization. The refractory sulfur adsorption performance of faujasite (FAU) zeolites, especially NaY and transition metal ion-exchanged Y zeolites, in model and real fuels has been widely investigated.[10−15] FAU zeolites possess higher adsorption capacity than other zeolitic types due to well-defined three-dimentional channels with a large pore opening of 7.4 × 7.4 Å, supercage cavity of 11.0 × 13.0 Å, and large amount of cation-exchangeable sites. However, high Al content results in low hydrothermal stability. Ultrastable Y (USY) is a FAU zeolite commercially prepared by high temperature steaming of ammonium-form or proton-form Y zeolite. Unlike NaY, it contains Brønsted and Lewis acid sites, additional weakly acidic hydroxyl groups, and various species of extra-framework aluminum (EFAL).[16−20] Despite a high surface area, the presence of secondary mesopores was reported.[21] Although USY has lower framework Al as well as smaller amount of framework cation-exchanged sites, its adsorption capacity toward DBT removal is higher than that of HY and 13X,[10] reflecting the influence of physicochemical properties of different FAU zeolites on the adsorption of thiophenic sulfurs.

Regarding the structure of TH, consisting of one lone pair of electrons on the sulfur atom and delocalized electrons on π bonds of the aromatic ring, the adsorption on a metal cation can occur either via a direct interaction at the sulfur atom or a π-complexation with the aromatic ring, depending on the type of the cation sites.[22] As a result, at least eight possible coordination geometries of TH−metal ion complexes can be formed, including two types of direct S−M bonding (η^1S and Sμ^3), four types of π-electronic interactions (η^4, η^5, η^2, and η^1C), and two modes of mixed interaction (η^4, Sμ^2 and η^4, Sμ^3).[23−25] The structure of aromatic sulfur has been found to significantly alter the HDS pathways, that is, direct hydrogenolysis or hydrogenation, over MoS_2-based catalysts.[26] The presence of additional benzene rings and methyl groups alters electron density on the sulfur atom and the bond order,[27] which may result in different adsorption modes on the catalysts. However, influences of thiophenic sulfur structures on the liquid-phase adsorption capacity and mechanism are still unclear.

The objective of present work is to study the influence of type of FAU zeolites and molecular structure of aromatic sulfurs on the adsorptive removal of TH, BT, and DBT from model fuel over Y and USY with different mono-, di-, and trivalence metal cations at ambient temperature and pressure. This is the first time that the effect of EFAL in USY zeolite on the adsorption has been elucidated. The influence of other aromatic compounds on the sulfur removal is also investigated to reveal

* To whom correspondence should be addressed. E-mail: chawalit.ng@chula.ac.th.

10.1021/ie701785s CCC: $40.75
Published on Web 09/06/2008

adsorption selectivity. In addition, the adsorptive desulfurization of real fuel and the reusability test for zeolitic adsorbents are studied.

Experimental Section

Adsorbent Preparation. Commercial NaY (Si/Al = 2.39) and HUSY (Si/Al = 3.06) zeolites were donated by Tosoh Corporation, Japan. To dealuminate the parent HUSY, typically an aqueous solution of HNO_3 with different concentrations was used. The solid-to-liquid ratio was maintained at 1:40. The adsorbents with desired Al contents were achieved by varying reaction temperature and time. The dealuminated HUSY was recovered by filtration, washed many times with deionized water, dried at 100 °C overnight, and calcined at 450 °C for 4 h.

Ion-exchanged zeolites were prepared by using various divalent and trivalent metal precursors (AR grade). In the cation-exchange of NaY, nitrate precursors, including $Cu(NO_3)_2 \cdot 2.5H_2O$, $Ni(NO_3)_2 \cdot 6H_2O$, $Zn(NO_3)_2 \cdot 6H_2O$, and $La(NO_3)_3 \cdot 6H_2O$, were used, whereas $NaOOCCH_3 \cdot 3H_2O$, $Cu(OOCCH_3)_2 \cdot H_2O$, $Ni(OOCCH_3)_2 \cdot 4H_2O$, $Zn(OOCCH_3)_2 \cdot 4H_2O$, and $La(NO_3)_3 \cdot 6H_2O$ were applied to the preparation of cation-exchanged HUSY. A zeolitic material calcined at 450 °C for 2 h was dispersed in a 0.1 M aqueous solution of metal precursor. The pH of the solution was controlled in the range of 6−7. The liquid/solid ratio was kept constant at 200. The slurry was stirred at ambient temperature and pressure for 24 h. Then, the solid product was recovered by filtration and thoroughly washed with deionized water, followed by drying at 100 °C overnight. Before being used in the adsorption experiment, it was calcined in a muffle furnace at 450 °C for 2 h. In some cases, the cation exchange procedure was repeated to increase the amount of metal ions.

Adsorbent Characterization. The crystallinity and unit cell parameter (a_0) of the parent, dealuminated, and cation exchanged zeolites were confirmed by using a Bruker D8 advanced X-ray diffractometer. Elemental analysis was by X-ray fluorescence spectroscopy (XRF) performed on a Siemens SRS3400 to determine type and amount of cation exchanged on zeolites. N_2 adsorption−desorption isotherm was measured on a Micromeritics ASAP 2020 surface area and porosity analyzer to investigate the change in surface area, pore size, and pore volume of zeolites by ion exchanging.

Extent of dealumination was confirmed by technique of inductively coupled plasma (ICP) spectroscopy. Fourier transform infrared (FTIR) spectra of USY before and after dealumination were recorded on a Perkin-Elmer 1600 FTIR spectrometer with a spectral resolution of 2 cm^{-1}. A 30-mg sample was pressed into a self-supported, 20-mm-diameter wafer. The wafer was set in a quartz infrared cell sealed with CaF_2 windows and connected to a vacuum system. The spectra were collected at room temperature in the absorbance mode with 64 scan times. To estimate the framework composition of HUSY, ^{29}Si MAS NMR spectra were recorded on a JEOL-LA WB 400 Hz spectrometer at 79.4 MHz and a sample spinning frequency of 5 kHz.

Adsorptive Desulfurization. Three model liquid fuels were used in the present study: 500 ppm TH (AR grade, Aldrich) in hexane, 500 ppm BT (AR grade, Aldrich) in hexane, and 500 ppm DBT (AR grade, Aldrich) in hexadecane. All chemicals were used without further purification. Commercial high-speed diesel with a sulfur concentration of 229 ppm purchased from Shell Thailand, Co., Ltd. was also used for studying the adsorption capacity and selectivity of adsorbents in the desulfurization of real fuel.

Table 1. Elemental Composition of Cation-Exchanged Y and HUSY Zeolites by Using the XRF Technique

adsorbent[a]	cation type	amount of cation exchanged in zeolite (mmol g^{-1})	molar ratio		
			Si/Al	M/Al[b]	Na/Al
NaY	Na^+	5.74[c]	2.48	1.37	1.37
CuNaY (IE-1)	Cu^{2+}	1.30	2.48	0.32	0.35
CuNaY (IE-2)	Cu^{2+}	1.83	2.48	0.46	0.3
NiNaY (IE-1)	Ni^{2+}	1.28	2.51	0.32	0.42
NiNaY (IE-2)	Ni^{2+}	1.41	2.46	0.34	0.38
ZnNaY (IE-1)	Zn^{2+}	1.68	2.48	0.4	
ZnNaY (IE-2)	Zn^{2+}	1.93	2.48	0.46	
LaNaY (IE-2)	La^{3+}	1.14	2.51	0.32	0.65
HUSY	H+		3.06		
NaHUSY (IE-2)	Na+	1.55	3.08	0.39	0.39
CuHUSY (IE-2)	Cu^{2+}	1.67	3.11	0.57	
NiHUSY (IE-2)	Ni^{2+}	1.50	3.12	0.52	
ZnHUSY (IE-2)	Zn^{2+}	1.88	3.09	0.54	
LaHUSY (IE-2)	La^{3+}	0.94	3.13	0.23	

[a] IE-1 = ion exchanged one time; IE-2 = ion exchanged twice. [b] M/Al represents the cation/aluminum molar ratio. [c] Amount of exchangeable sodium ion.

The batch adsorption experiment was carried out at ambient temperature and pressure. Typically, 1 g of calcined adsorbent was added into a liquid fuel in a 100-mL glass vial. The liquid fuel/adsorbent weight ratio was varied in the range 10−100. The mixture was stirred vigorously for 24 h. The adsorbent was separated by filtration. The amount of aromatic sulfurs remaining was analyzed with a Varian CP3800 gas chromatograph equipped with a 30-m DB-1HT capillary column and a FID detector. Response of the detector within the studied range of sulfur concentration was linear as revealed by calibration curves of the three sulfur compounds. In the case of adsorptive desulfurization of real fuel, the amount and type of refractory sulfurs remaining were analyzed by XRF with a Siemens SRS3400 and a Hewlett-Packard HP6890 gas chromatograph with a FPD detector, respectively. The amount of sulfurs removed (wt %) was calculated as follows:

$$\text{sulfur removal (wt \%)} = \frac{\text{initial S concentration (ppm)} - \text{final S concentration (ppm)}}{\text{initial S concentration (ppm)}} \times 100 \quad (1)$$

Results and Discussion

Characterization of Cation-Exchanged FAU Zeolites. Table 1 shows elemental composition and amount of cation in NaY and HUSY before and after the cation exchange. It can be seen that the Si/Al ratio of NaY exchanged once (IE-1) and twice (IE-2) was not significantly different from that of the parent NaY, indicating that there was a small degree of dealumination during the cation exchange step. Moreover, the amount of metal ions increased with the repetition of ion exchanging. Theoretically, one divalent metal ion balances negative charges generated from two framework Al atoms (2 × M/Al). From Table 1, ion-exchanged capacity for each metal in once and twice exchange is as follows: $2Cu^{2+}/Al^{3+} = 0.64$, 0.92; $2Ni^{2+}/Al^{3+} = 0.64$, 0.68; and $2Zn^{2+}/Al^{3+} = 0.80$, 0.92. Therefore, Na can be exchanged for Zn the most and for Ni the least. In the case of exchanging for La^{3+}, one La^{3+} theoretically balances three negative charges from three framework Al (3 × M/Al). Thus, the Na-exchanged capacity for La^{3+} was 96%.

Compared with the analysis results of NaY, the amount of cation exchanged in HUSY was lower because the Si/Al ratio of HUSY is higher than that of NaY, resulting in a lower amount

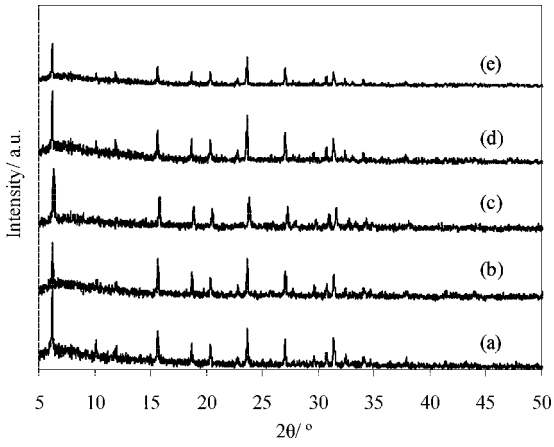

Figure 1. XRD patterns of NaY (a), CuNaY (b), NiNaY (c), ZnNaY (d). and LaNaY (e).

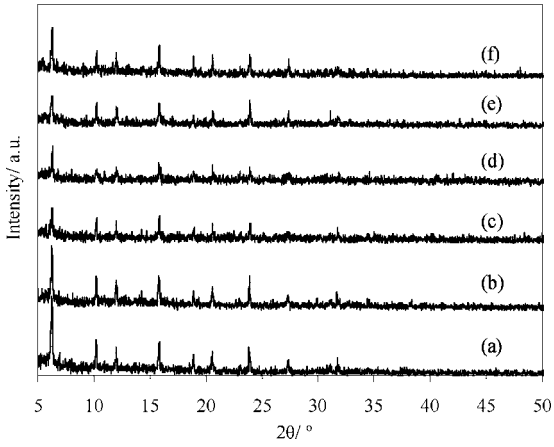

Figure 2. XRD patterns of HUSY (a), NaHUSY (b), CuHUSY (c), NiHUSY (d), ZnHUSY (e), and LaHUSY (f).

of cation exchange sites. In addition, the presence of EFAL, as cation species[17,18] and/or alumina debris,[19,20] can block the ion exchange sites and hamper the exchanging process. It can be seen that, after the ion exchange, the Si/Al ratio of HUSY was significantly increased. This should account for the leaching of EFAL. Moreover, the ion-exchanged capacity for divalent metal ions in this case slightly exceeded 100%. This result may be derived from the complexity of Al species in HUSY zeolite.

Figure 1 illustrates XRD patterns of calcined NaY before and after ion exchanging. The major characteristic peaks of FAU type zeolite remained after the ion exchange with Cu^{2+}, Ni^{2+}, and Zn^{2+}, indicating that the structure of parent NaY was not significantly damaged. However, NaY ion-exchanged with La^{3+} solution exhibited a remarkable decrease in the peak intensity. It might be due to a strong Lewis acid character of this ion, enhancing the degree of dealumination as suggested by a slight increase in the Si/Al ratio of LaNaY (Table 1).

XRD patterns of calcined HUSY before and after ion exchanging are revealed in Figure 2. There was a significant change in the intensity of diffraction peaks after the ion exchange, suggesting a loss of crystallinity. This result is consistent with the XRF result presented in Table 1. It indicated the occurrence of dealumination during the ion exchange. It is also worth noting that, in all cases, there was no the formation of oxides derived from divalent and trivalent introduced to the zeolites, as confirmed by the XRD analyses.

The presence of EFAL can also influence the adsorption capacity of HUSY and its derivative adsorbents. Table 2 reveals the dealumination conditions of HUSY and the structural properties of HUSY and dealuminated USY (DeHUSY) zeolites. After the dealumination, the bulk Si/Al ratio was increased concomitantly with a decrease in the amount of EFAL. Using 0.1 M HNO_3 solution (DeHUSY-1) was not harmful to the FAU structure as evidenced by a retention of crystallinity, unit cell constant, and amount of framework Al (FAL). When HUSY was dealuminated by 0.2 M HNO_3 (DeHUSY-2), EFAL could be removed at higher extent concomitantly with some loss of crystallinity and the decrease in the amount of FAL.

FTIR spectra of HUSY and dealuminated HUSY zeolites in the O−H stretching region are compared in Figure 3. The bands at 3628 and 3564 cm^{-1} are the characteristic O−H vibration of Brønsted acid sites located in supercages and sodalite cages, respectively. The band at 3740 cm^{-1} was associated with silanol groups (Si−OH), and the band around 3670 cm^{-1} was assigned to Al−OH groups of EFAL species.[28] The band at 3600 cm^{-1} was attributed to Brønsted acid sites coordinated with EFAL in supercages.[28] The spectrum of DeHUSY-1 (Figure 3b) was similar to that of parent HUSY (Figure 3a) but with a slight improvement of band intensity. The combined results from Table 3 and Figure 3 suggested that the treatment conditions for DeHUSY-1 can remove extra-framework species, such as amorphous silica−alumina phase and/or debris.[29,30] However, a significant amount of electron-deficient EFAL species, related to the band at 3600 cm^{-1}, still remained, suggesting their strong coordination with the zeolitic framework. In the case of DeHUSY-2 (Figure 3c), a large amount of silanol groups was formed, possibly via the hydrolysis of some EFAL species as well as the dealumination of FAL.

Influence of Type and Amount of Cations on Adsorptive Desulfurization over Cation-Exchanged FAU Zeolites. Table 3 shows TH removal of model fuel over various Y adsorbents with different cation types and amounts. The adsorption experiment was carried out at ambient temperature and pressure with the liquid fuel/adsorbent weight ratio of 10. Compared with the parent NaY, the adsorption capacity of NaY exchanged with Cu^{2+} and Ni^{2+} was enhanced. The TH removal was increased from 67.6 to 70.8 and 80.6%, respectively. In contrast, ZnNaY did not exhibit any adsorption improvement. Its adsorption capacity (66.2%) was comparable to that of NaY. This result agrees with the previous work.[13] Cu^{2+} has higher energy for TH adsorption than Ni^{2+} and Zn^{2+}. With the repetition of ion exchange, the amount of cation was increased (Table 1), resulting in an enhancement of TH removal. The sequence of adsorption capacity among these Y-type adsorbents was still the same. CuNaY exhibited the highest adsorption capacity at 90% TH removal, corresponding to 4.54 mg of S/g of adsorbent. Among USY adsorbents, the TH removal was decreased in the following order: CuHUSY > NiHUSY > ZnHUSY > NaHUSY > HUSY (Table 3). This result is consistent with the adsorption over Y-type adsorbents. The twice exchanged CuHUSY possessed the highest TH removal of 69%, corresponding to 3.45 mg of S/g of adsorbent.

Table 3 presents the results of the effect of cation charges on the TH adsorption. For the Y series, the TH removal was increased in the following order: $Na^+ < Cu^{2+} < La^{3+}$. Among USY members, the adsorption capacity increased in the order $H^+ < Cu^{2+} < La^{3+}$. The high adsorption capacity of both La^{3+}-FAU zeolites should be attributed to the high positive charge of La^{3+} itself that can enhance the adsorption of TH molecules via the direct interaction.[15] The calculated amount of TH removed was 5.44 and 4.43 mg of S/g of adsorbent for LaNaY and LaHUSY, respectively.

Table 2. Treatment Conditions and Structural Properties of HUSY and Dealuminated HUSY Zeolites

	treatment conditions						Al per unit cell			
zeolite	acid solution	temperature (°C)	time (h)	crystallinity[a] (%)	unit cell[b] a_0 (Å)	bulk[c] Si/Al	FAL[d]	EFAL[e]	framework[f] Si/Al_{XRD}	framework[g] Si/Al_{SiNMR}
HUSY				100	24.37	3.5	16.7	26.0	10.5	11.8
DeHUSY-1	0.1 M HNO_3	80	3	107	24.37	5.5	16.7	12.8	11.5	16.7
DeHUSY-2	0.2 M HNO_3	25	2	89	24.31	12.0	9.8	5.0	18.6	18.6

[a] Relative to XRD pattern of the parent HUSY. [b] Calculated from the diffraction peak corresponding to (533) reflection plane. [c] From chemical analysis by ICP. [d] FAL means framework Al. Calculated from XRD analysis using Beyer's equation. [e] EFAL means extra-framework Al. Calculated from difference between the amount of bulk Al and that of FAL. [f] Using FAL obtained from XRD analysis. [g] From ^{29}Si MAS NMR.

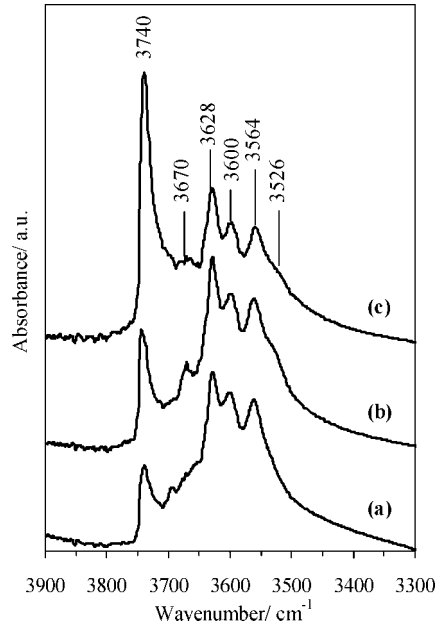

Figure 3. FTIR spectra of HUSY (a), DeUSY-1 (b), and DeUSY-3 (c) in the O−H stretching region.

Table 3. TH Adsorption[a] of Various Cation-Exchanged NaY and HUSY

adsorbent[b]	amount of TH remaining after adsorption (ppm)	TH removal (wt %)	adsorption capacity (mg of S/g of adsorbent)
NaY	162	67.6	3.38
NiNaY (IE-1)	146	70.8	3.54
NiNaY (IE-2)	108	78.4	3.92
CuNaY (IE-1)	97	80.6	4.03
CuNaY (IE-2)	46	90.8	4.54
ZnNaY (IE-1)	169	66.2	3.31
ZnNaY (IE-2)	148	70.4	3.52
LaNaY (IE-2)	28	94.4	4.72
HUSY	350	30.0	1.50
NaHUSY (IE-2)	285	43.0	2.15
NiHUSY (IE-2)	195	61.0	3.05
CuHUSY (IE-2)	154	69.2	3.45
ZnHUSY (IE-2)	240	52.0	2.60
LaHUSY (IE-2)	116	76.8	3.84
DeHUSY-1[c]	329	34.2	1.71
DeHUSY-2	341	31.8	1.59

[a] Adsorption conditions: initial sulfur concentration, 500 ppm; liquid/solid weight ratio, 10; ambient temperature and pressure. [b] IE-1 = ion exchanged one time; IE-2 = ion exchanged twice. [c] DeHUSY means dealuminated HUSY.

The TH adsorption test over both dealuminated HUSY zeolites is also revealed in Table 3. DeHUSY-1 exhibited higher TH removal than DeHUSY-2 due to the higher FAL content (Table 2). However, there was no remarkable improvement of the adsorption capacity after removing some nonframework silica−alumina phase. It should be ascribed to the amount of these EFAL species that is not significant to increase the amount of cation exchangeable sites. In addition, some amorphous silica−alumina species confer Lewis acidity of different strengths[30−33] and can behave like adsorption sites. The removal of these species may inversely reduce the adsorption capacity, even though the amount of cation exchangeable sites increases.

Influence of Molecular Structure of Aromatic Sulfurs on Adsorptive Desulfurization over Cation-Exchanged FAU Zeolites. To study the effect of molecular structure of adsorbate, aromatic sulfurs with different molecular sizes, TH, BT, and DBT, were selected as representative sulfur molecules in the model fuels. Figure 4 illustrates the molecular size and dimension of each representative aromatic sulfur estimated from CambridgeSoft Chem 3D program using energy minima and MM2 field. Normally, FAU zeolites possess three-dimensional channels with a pore aperture of 7.4 × 7.4 Å. From the molecular structure of the sulfur compounds, each thiophenic sulfur with an appropriate orientation can diffuse into the zeolitic pores of both Y and USY adsorbents.

As shown in Figure 5, it is interesting that, on both zeolites, DBT with the largest molecular size was adsorbed at the highest amount, while the removal of TH with the smallest size was the lowest. This result should account for the presence of additional aromatic rings in BT and DBT, which enhance probability to form π-electronic interaction on the cation sites. Moreover, Ma et al. reported an increase in the electron density at the sulfur atom of thiophenic sulfurs in the following order: TH (5.696) < BT (5.739) < DBT (5.758).[27] The increase in the electron density probably enhances the direct interaction between the metal ions and the refractory sulfur molecules. It is worth noting that although NaY had much higher TH adsorption capacity than HUSY, the capacity difference in the adsorption of BT and DBT was remarkably reduced. This result can be explained by the nature of cationic species that alters the adsorption mechanism in the presence of aromatic sulfurs with different molecular structures.

Figures 6 and 7 illustrate adsorption isotherms of BT and DBT, respectively, on NaY and HUSY zeolites. The TH adsorption isotherms for FAU-type zeolites were similar to those reported in the literature.[10] In that case, NaY exhibited type V isotherm, typically for mutilayer adsorption, while HY and USY showed the isotherms of Langmuir adsorption.[10] This result suggested that TH is adsorbed on the proton-form zeolites with more specific and stronger interaction than on NaY. It should be related to the fact that Na^+ can interact with aromatic sulfurs via both direct and π-electronic adsorption, while H^+ with high positive charge density favors the direct interaction more than relatively weak π-electronic interaction.

It was found that the adsorption of BT (Figure 6) and DBT (Figure 7) on both NaY and HUSY zeolites revealed the isotherms of type V, suggesting that the interaction of both TH derivatives on zeolites became weaker compared with the TH adsorption. The flow calorimetric study on the adsorption of

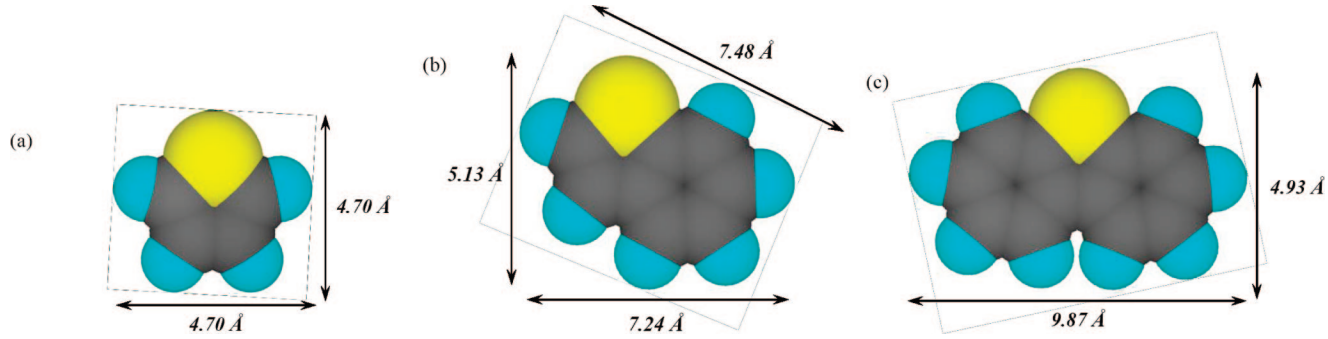

Figure 4. Molecular dimensions of TH (a), BT (b), and DBT (c) estimated by using CambridgeSoft Chem 3D program.

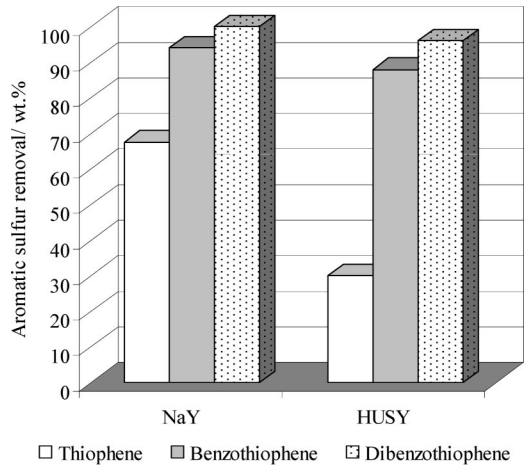

Figure 5. Comparison of TH, BT, and DBT removal over NaY and HUSY.

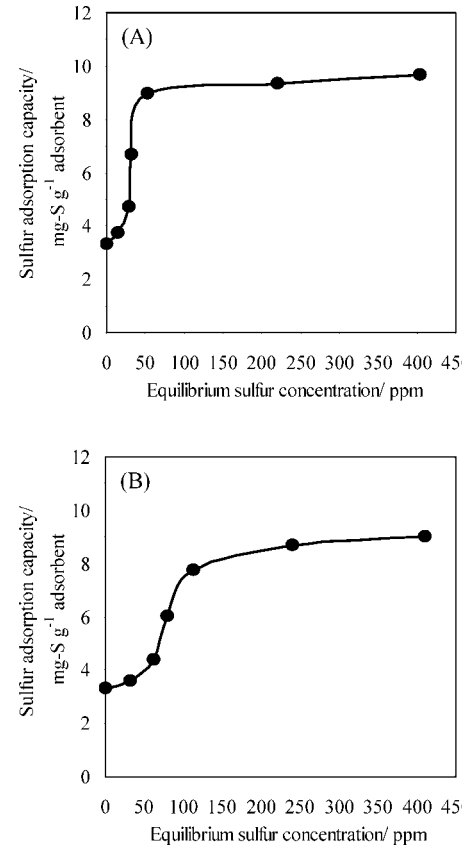

Figure 6. Adsorption isotherms for BT removal over NaY (A) and HUSY (B) at ambient temperature.

various thiophenic sulfur compounds indicated an increase in the heat of adsorption in the order 4,6-dimethyldibenzothiophene (4,6-DMDBT) < DBT < BT < TH.[10] These results implied that the π-electronic interaction plays a more important role in both cases, even though this adsorption mechanism is more favored by the adsorption on Na^+ as also reflected by faster increase in the adsorption capacity in the isotherms of NaY (Figures 6A and 7A).

Figure 8 shows BT and DBT removal of the model fuel on NaY and HUSY ion-exchanged with Cu^{2+} and La^{3+}. The result of TH adsorption is also present for comparison. As a result of the high adsorbed amount and small difference in the adsorption capacity of parent NaY and HUSY (Figure 5), the liquid fuel/adsorbent weight ratio in this study was increased to 100. Regarding to the cation type, the trend of BT adsorption capacity was similar to the TH adsorption. However, it is interesting that LaHUSY zeolite possessed the highest BT removal, 30.4 wt %, corresponding to 15.17 mg of S/g of adsorbent, while LaNaY exhibited the highest TH adsorption capacity. This result should be related to the larger size of BT than TH (Figure 4). It can be noted that USY-type zeolite usually has defect sites and some mesopores generated during the steam treatment and acid washing,[21] resulting in larger average pore volume compared with the parent Y. From N_2 adsorption−desorption measurement, HUSY had pore volume of 0.47 $cm^3\ g^{-1}$, while the pore volume of NaY was 0.34 $cm^3\ g^{-1}$. Therefore, the adsorption of BT can be facilitated by these large pores in HUSY adsorbents.

For the DBT adsorption over USY adsorbent series, it can be seen that the trend of adsorption capacity was similar to the case of TH and BT adsorption, where LaHUSY showed the highest adsorption capacity, 87.8% corresponding to 43.87 mg of S/g of adsorbent. However, for the series of NaY adsorbents, CuNaY exhibited the highest DBT removal, 93.8% corresponding to 46.90 mg of S/g of adsorbent. These results should be attributed to the molecular structure of DBT and pore size of the zeolites.

The large molecular size of DBT (Figure 4) renders its movement inside the zeolitic pores relatively difficult. As mentioned above, NaY zeolite has relatively small pore volume compared to USY, and La^{3+} enhances the direct adsorption at the sulfur atom.[15] So, it is rather difficult for DBT to orient into an appropriate direction to form direct interaction with La^{3+} in NaY. On the contrary, Cu^{2+} can exhibit the π-electronic adsorption with the aromatic rings of the DBT molecule. There are more possible orientations to form such an interaction. This resulted in the higher DBT adsorption capacity of CuNaY than that of LaNaY. When more spaces are available in zeolite pores, the direct interaction with La^{3+} is more possible in HUSY and the DBT adsorption was enhanced over LaHUSY zeolite.

Influence of Aromatic Compounds on Adsorptive Desulfurization over Cation-Exchanged FAU Zeolites. Tables 4−6 reveal the effect of other aromatic compounds in model

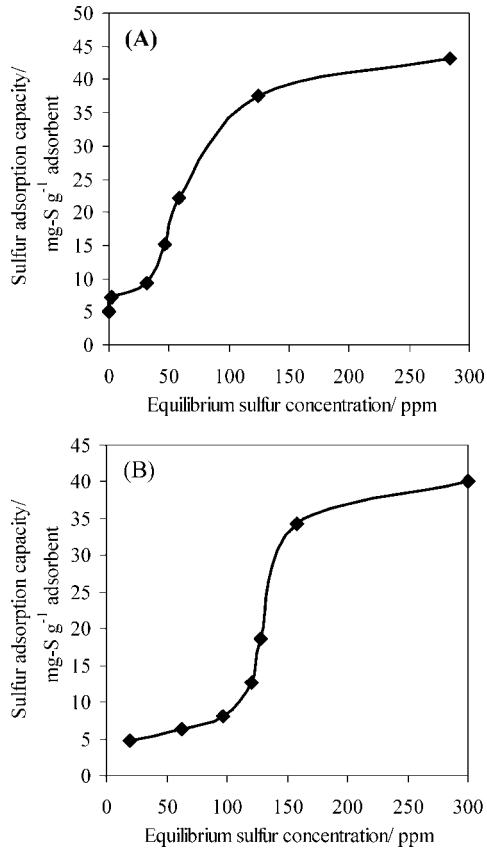

Figure 7. Adsorption isotherms for DBT removal over NaY (A) and HUSY (B) at ambient temperature.

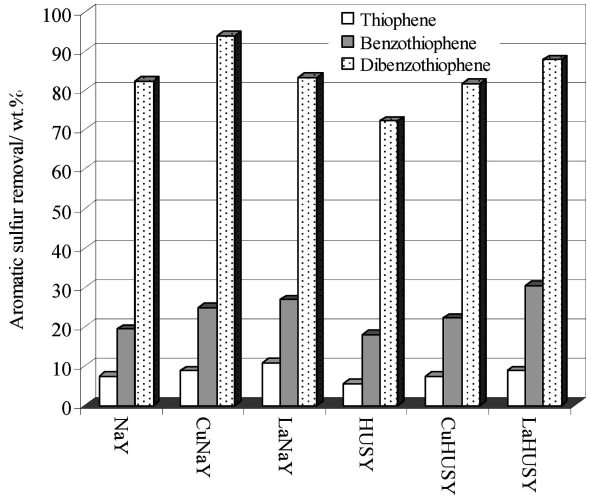

Figure 8. TH, BT, and DBT removal over various Y and USY adsorbents.

fuel on the refractory sulfur removal over cation-exchanged Y and USY zeolites. Benzene rings of toluene and naphthalene, as model aromatic compounds, can interact with the cation sites using π electrons.

It was found that, in the presence of 500 ppm toluene (Table 4) or naphthalene (Tables 5 and 6), the removal of refractory sulfurs was decreased. These results should be ascribed to the competitive adsorption between the sulfur molecules and the aromatic compounds.[11] Similarly to the trend of adsorption results in the absence of aromatic compounds, LaNaY showed the highest adsorption capacity, 4.49 mg of S/g of adsorbent, for TH removal (Table 4), while LaHUSY exhibited the highest

Table 4. TH Removal[a] in the Presence of Toluene over Cation-Exchanged Y and USY Zeolites

	amount adsorbed (mmol g^{-1})		TH removal (wt %)		
adsorbent[b]	TH	toluene[c]	with toluene	without toluene	sulfur adsorption capacity (mg of S/g of adsorbent)
CuNaY	0.133	0.048	85.2	90.8	4.26
LaNaY	0.140	0.037	89.8	94.4	4.49
CuHUSY	0.101	0.040	64.4	69.2	3.22
LaHUSY	0.115	0.036	73.6	76.8	3.68

[a] Adsorption conditions: initial sulfur concentration, 500 ppm; liquid fuel/adsorbent weight ratio, 10; ambient temperature and pressure. [b] Ion exchanged twice. [c] The initial toluene concentration was 500 ppm.

Table 5. BT Removal[a] in the Presence of Naphthalene over Cation-Exchanged Y and USY Zeolites

	amount adsorbed (mmol g^{-1})		BT removal (wt %)		
adsorbent[b]	BT	naphthalene[c]	with naphthalene	without naphthalene	sulfur adsorption capacity (mg of S/g of adsorbent)
CuNaY	0.205	0.080	39.4	80.7	6.57
LaNaY	0.211	0.069	40.6	82.0	6.75
CuHUSY	0.188	0.076	36.0	69.8	6.00
LaHUSY	0.224	0.064	43.0	83.9	7.16

[a] Adsorption conditions: initial sulfur concentration, 500 ppm; liquid fuel/adsorbent weight ratio, 33.3; ambient temperature and pressure. [b] Ion exchanged twice. [c] The initial naphthalene concentration was 500 ppm.

Table 6. DBT Removal[a] in the Presence of Naphthalene over Cation-Exchanged Y and USY Zeolites

	amount adsorbed (mmol g^{-1})		DBT removal (wt %)		
adsorbent[b]	DBT	naphthalene[c]	with naphthalene	without naphthalene	sulfur adsorption capacity (mg of S/g of adsorbent)
CuNaY	0.769	0.201	49.2	93.8	24.6
LaNaY	0.506	0.191	32.4	82.7	16.2
CuHUSY	0.765	0.208	49.0	81.9	24.5
LaHUSY	0.893	0.202	57.2	87.8	28.6

[a] Adsorption conditions: initial sulfur concentration, 500 ppm; liquid fuel/adsorbent weight ratio, 100; ambient temperature and pressure. [b] Ion exchanged twice. [c] The initial naphthalene concentration was 500 ppm.

capacity, 7.16 mg of S/g of adsorbent, for BT adsorption (Table 5). Moreover, it can be seen that the amount of toluene or naphthalene adsorbed was lower in the case of LaNaY and LaHUSY, indicating that the adsorption of both thiophenic sulfurs on La^{3+}-exchanged adsorbents is more selective than that on divalent ion-exchanged ones. It should be due to the highly positive charge of La^{3+} that is capable of forming relatively strong direct interaction with the sulfur atom of both thiophenic compounds.

As a result of the competitive adsorption, the DBT removal was greatly reduced to 49.2% for CuNaY, 32.4% for LaNaY, 49.0% for CuHUSY, and 57.2% for LaHUSY (Table 6). This trend was different from the case of adsorption without naphthalene. In the presence of naphthalene, LaHUSY possessed the smallest decrease in DBT removal (57.2%) corresponding to the highest sulfur adsorption capacity of 28.6 mg of S/g of adsorbent, whereas CuNaY exhibited the highest DBT removal (93.8%) when naphthalene was absent. It should be related to the bulky size of both DBT and naphthalene. Once naphthalene was adsorbed inside the zeolitic pores, the available space for accommodation of DBT molecules was decreased. Therefore, LaHUSY providing larger pore size and higher pore volume concomitantly with high electron deficient La^{3+} can adsorb DBT at the highest amount. The DBT removal over LaNaY was

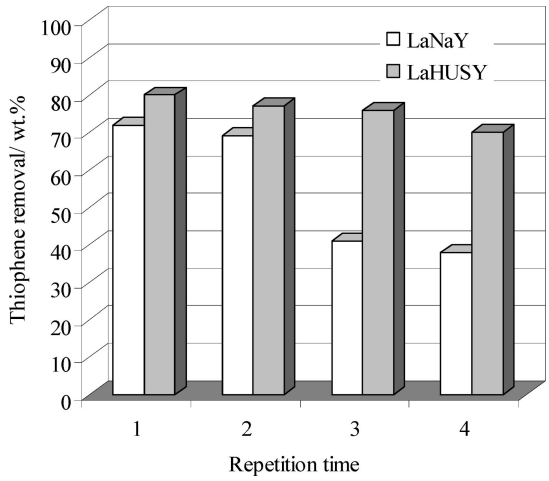

Figure 9. Reusability of LaNaY and LaHUSY in TH removal.

decreased at the highest extent (from 82.7 to 32.4%), and the total adsorbed amount was lowest at 0.506 mmol g^{-1} among the adsorbents studied. This should be due to relatively small pore volume of NaY and low crystallinity of LaNaY as evidenced by the XRD pattern (Figure 1).

It is worth noting that the selectivity toward naphthalene adsorption on both the Y and the USY series was not obviously different. All of the cation-exchanged zeolites adsorbed naphthalene at comparable amounts, approximately 0.200 mmol g^{-1}. These results are different from the results obtained from the TH and BT adsorption in Tables 4 and 5. As discussed in the previous section, the bulky size of DBT and the presence of two aromatic rings in the molecule enhance the π-electronic interaction on the cation sites. Thus, DBT was competitively adsorbed with naphthalene in the similar mode. Nevertheless, as a result of La^{3+} characteristics, we observed the slightly lower amount of naphthalene adsorbed over La^{3+}-FAU zeolites.

Reusability Test of La^{3+}-FAU Adsorbents. To test the reusability of LaNaY and LaHUSY, after the adsorption of TH in *n*-hexane in the first run, both adsorbents were recovered by filtration, followed by washing with *n*-hexane, air drying, and calcination at 450 °C for 4 h in a muffle furnace. From Figure 9, the TH removal of both adsorbents was slightly decreased in the second repetition (2−3%). However, in the third and fourth repetitions, the removal of TH over LaNaY was remarkably decreased to 39 and 35%, respectively. As a well-known phenomenon, NaY is sensitive to water, especially at high temperatures.[34] A small amount of water generated during combustion of organic compounds remaining in the adsorbent can damage its zeolitic structure via dealumination. However, USY (ultrastable Y) is a hydrothermal stable form of FAU zeolite. Therefore, the TH removal as high as 68% can be attained over LaHUSY in the fourth repetition. These results revealed that LaHUSY has a high stability toward thermal regeneration and can be used for more repetition times.

Adsorptive Desulfurization of Real Fuel over Cation-Exchanged FAU Zeolites. For desulfurization of real fuel, the adsorption capacity and selectivity of NaY and HUSY and their cation-exchanged series were investigated. Diesel, one of the major fuels in the Thailand transportation sector, was chosen. The commercial diesel from Shell (Thailand) Co., Ltd., with the initial sulfur concentration of 229 ppm was used. According to EURO4 regulation,[4] the target sulfur limit in the resultant diesel must be less than 50 ppm. The adsorption was carried out batchwise at ambient temperature and pressure, and the diesel/adsorbent weight ratio was kept constant at 100.

Table 7. Adsorptive Desulfurization[a] of Commercial Diesel over Various Cation-Exchanged Y and USY Zeolites

adsorbent[b]	amount of sulfur remaining after adsorption (ppm)	sulfur removal (wt %)
NaY	196	14.4
CuNaY	191	16.6
LaNaY	193	15.7
HUSY	203	11.4
CuHUSY	187	18.3
LaHUSY	180	21.4

[a] The diesel/adsorbent weight ratio was 100, and the initial sulfur concentration in diesel was 229 ppm. [b] Ion exchanged twice.

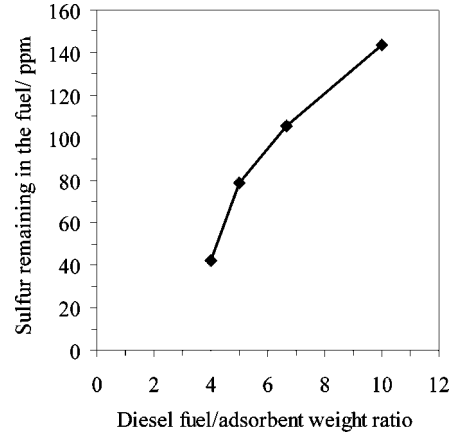

Figure 10. Influence of liquid fuel/adsorbent weight ratio on sulfur removal from real diesel.

The preliminary results from desulfurization of diesel over NaY, CuNaY, LaNaY, HUSY, CuHUSY, and LaHUSY are presented in Table 7. It can be seen that LaHUSY exhibited the highest sulfur removal of 21.4%. This result is consistent with the competitive adsorption of DBT and naphthalene in Table 6. Compared to the case of model fuels (Table 6), the sulfur removal of real diesel was much lower. It should be related to the presence of various aromatic compounds, such as naphthalene derivatives (suggested by GCMS analysis of the real diesel), resulting in the competitive adsorption on cation sites. It can be seen that the influence of cation types on the adsorption over USY series was stronger than that over Y adsorbents. The smaller pore volume of the latter may limit uptake of refractory sulfur compounds. At these experimental conditions, LaHUSY is the best adsorbent, probably due to the stronger interaction of sulfur atom and La^{3+} in the direct adsorption and more spaces available within the USY structure.

To reduce the sulfur level in diesel to less than 50 ppm, the diesel/adsorbent ratio was varied to find a suitable condition. Figure 10 shows the sulfur removal over LaHUSY zeolite at various diesel/adsorbent ratios. It was found that the sulfur level in diesel after the adsorption decreased with decreasing the ratio (increasing the amount of adsorbent). At the diesel/adsorbent weight ratio of 4, the sulfur level was reduced to 42 ppm.

Figure 11 illustrates chromatograms from GC-FPD analyses of diesel before and after the adsorptive desulfurization over LaHUSY at the fuel/adsorbent ratio of 4. The initial diesel (Figure 11A) is composed of a small amount of DBT but higher amounts of its derivatives, mostly 4-methyldibenzothiophene (4-MDBT) and 3-methyldibenzothiophene (3-MDBT). More refractory sulfur compounds were also present, including 4,6-dimethyldibenzothiophene (4,6-DMDBT), 3,6-dimethyldibenzothiophene (3,6-DMDBT), and 2,4,6-trimethyldibenzothiophene (2,4,6-TMDBT). After the adsorption (Figure 11B), the amount

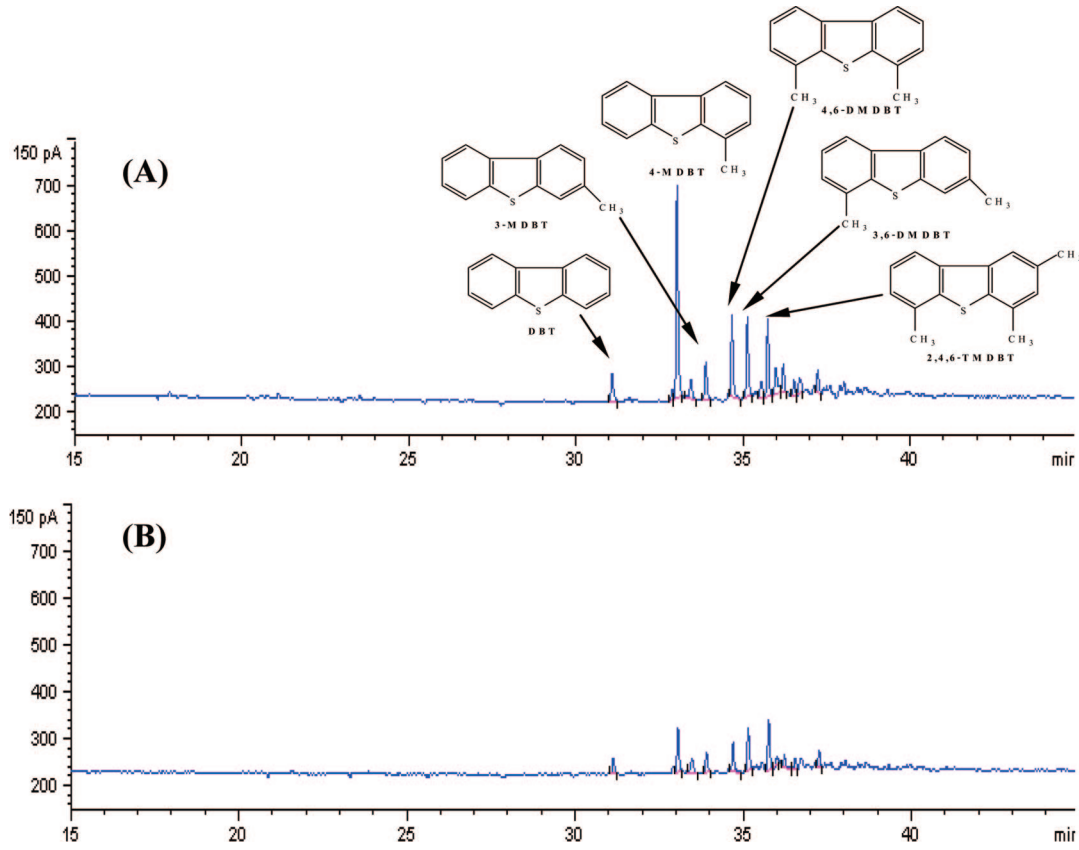

Figure 11. GC-FPD chromatograms of real diesel before (A) and after (B) adsorptive desulfurization over LaHUSY.

of all refractory sulfur species was obviously decreased. Adsorption selectivity to each aromatic sulfur compound, defined as

$$\text{adsorption selectivity} = \frac{\text{peak area before adsorption} - \text{peak area after adsorption}}{\text{total peak area before adsorption} - \text{total peak area after adsorption}} \quad (2)$$

was decreased in the following order: 4-MDBT > 4,6-DMDBT > 3,6-DMDBT > DBT ≈ 3-MDBT > 2,4,6-TMDBT. This result is in accordance with the quantum calculation result reported earlier that 4-MDBT possesses high electron density at the sulfur atom.[27] Kabe et al. proposed that 4-MDBT or 4,6-DMDBT can be adsorbed on the catalyst through a π-electron in the aromatic rings more strongly than DBT.[35] The effect of enhancement of electron density at sulfur atom and within aromatic rings by methyl substituents on the adsorption was also reflected from the higher selectivity to 4,6-DMDBT and 3,6-DMDBT than DBT. Regardless of molecular size, 3-MDBT exhibited the adsorption selectivity similarly to DBT. The methyl substituent at the 3-position may influence particularly the electron density in the benzene ring, resulting in a weakly direct interaction with La^{3+}. TMDBT is highly steric hinder molecule and has some difficulties to be adsorbed within the zeolite channels.

Conclusions

Cation-exchanged Y and USY zeolites, successfully prepared without a drastic loss of crystallinity and a formation of nonframework metal oxides, were applied as adsorbents for desulfurization of liquid fuels. With an increase in the cation amount, the TH removal was increased. Cu^{2+} exhibited the best divalent cation on both Y and USY zeolites. However, the highest TH removal was possessed by La^{3+}-exchanged adsorbents, which is promoted by a relatively strong direct interaction at the sulfur atom. The presence of EFAL did not much alter the adsorption unless the cation exchange sites were hindered. The adsorption capacity increased with the molecular size from TH to BT and DBT. The isotherms suggested that the adsorption mechanism was changed from direct to π-electronic interaction with increasing the size of thiophenic molecules. LaHUSY exhibited superior adsorption capacity for BT, while the removal of DBT was highest over CuNaY. The adsorption selectivity in the presence of other aromatic compounds was evident in the adsorption of TH and BT. When the π-electronic interaction was dominant in the DBT adsorption, the amount of naphthalene adsorbed was comparable regardless of cation type. The removal of refractory sulfurs from real diesel over LaHUSY was relatively high. The formulated adsorption selectivity in this case suggested that not only the molecular size but also the electron density at the sulfur atom and in the aromatic ring influenced by the methyl substituents determines the adsorption performance of zeolitic adsorbents.

Acknowledgment

The authors are grateful to the Asahi Glass Foundation, Japan, and the National Center of Excellence for Petroleum, Petrochemicals and Advanced Materials, Chulalongkorn University, for the financial support. The authors also thank the Tosoh Corporation, Japan, for donating the commercial zeolites.

Literature Cited

(1) Lee, S. L.; De Wind, M.; Desai, P. H.; Johnson, C. C.; Asim Mehmet, Y. Aromatics Reduction and Cetane Improvement of Diesel Fuels. *Fuel Reformulation* **1993**, *5*, 26.

(2) Unzelman, G. H. Fuel Projections and Technology Closer to Reality. *Fuel Reformation* **1993**, *5*, 38.

(3) Khan, M. R.; Reynolds, J. G. Formulating a Response to the Clean Air Act. *CHEMTECH* **1996**, *26*, 56.

(4) Sotelo, J. L.; Uguina, M. A.; Romero, M. D.; Gomez, J. M.; Agueda, V. I.; Ortiz, M. A. Dibenzothiophene Adsorption over Zeolites with Faujasite Structure. *Stud. Surf. Sci.* **2001**, *135*, 227.

(5) EPA-Diesel RIA. *Regulatory Impact Analysis: Heavy-Duty Engine and Vehicle Standards and Highway Diesel Fuel Sulfur Control Requirements*, EPA420-R-00-026; United States Environmental Protection Agency, Air and Radiation, December, 2000.

(6) Gerritsen, L. A. Production of Green Diesel in the BP Amoco Refineries. Presented by Akzo Nobel at the WEFA Conference, Berlin, Germany, June 2000.

(7) Yoosuk, B.; Kim, J. H.; Song, C.; Ngamcharussrivichai, C.; Prasassarakich, P. Highly Active MoS_2, $CoMoS_2$ and $NiMoS_2$ Unsupported Catalysts Prepared by Hydrothermal Synthesis for Hydrodesulfurization of 4,6-Dimethyldibenzothiophene. *Catal. Today* **2008**, *130*, 14.

(8) Song, C. An Overview of New Approaches to Deep Desulfurization for Ultra-clean Gasoline, Diesel Fuel and Jet Fuel. *Catal. Today* **2003**, *86*, 211.

(9) Song, C.; Ma, X. New Design Approaches to Ultra-clean Diesel Fuels by Deep Desulfurization and Deep Dearomatization. *Appl. Catal., B* **2003**, *41*, 207.

(10) Ng, F. T. T.; Rahman, A.; Ohasi, T.; Jiang, M. A Study of the Adsorption of Thiophenic Sulfur Compounds Using Flow Calorimetry. *Appl. Catal., B* **2005**, *56*, 127.

(11) Velu, S.; Ma, X.; Song, C. Selective Adsorption for Removing Sulfur from Jet Fuel over Zeolite-Based Adsorbents. *Ind. Eng. Chem. Res.* **2003**, *42*, 5293.

(12) Hernández-Maldonado, A. J.; Yang, R. T. Desulfurization of Commercial Liquid Fuels by Selective Adsorption via π-Complexation with Cu(I)-Y Zeolite. *Ind. Eng. Chem. Res.* **2003**, *42*, 3103.

(13) Hernández-Maldonado, A. J.; Yang, F. H.; Oi, G.; Yang, R. T. Desulfurization of Transportation Fuels by π-Complexation Sorbents: Cu(I)-, Ni(I)-, and Zn(II)-Zeolites. *Appl. Catal., B* **2005**, *56*, 111.

(14) Xue, M.; Chitrakar, R.; Sakane, K.; Hirotsu, T.; Ooi, K.; Yoshimura, Y.; Feng, Q.; Sumida, N. Selective Adsorption of Thiophene and 1-Benzothiophene on Metal Ion-Exchanged Zeolites in Organic Medium. *J. Colloid Interface Sci.* **2005**, *285*, 487.

(15) Tian, F.; Wu, W.; Jiang, Z.; Liang, C.; Yang, Y.; Ying, P.; Sun, X.; Cai, T.; Li, C. The Study of Thiophene Adsorption onto La(III)-Exchanged Zeolite NaY by FT-IR Spectroscopy. *J. Colloid Interface Sci.* **2006**, *301*, 395.

(16) Pöppl, A.; Rudolf, T.; Michel, D. A Pulsed Electron Nuclear Double Resonance Study of the Lewis Acid Site-Nitric Oxide Complex in Zeolite H-ZSM-5. *J. Am. Chem. Soc.* **1998**, *120*, 4879.

(17) Remy, M. J.; Stanica, D.; Poncelet, G.; Feijen, E. J. P.; Grobet, P. J.; Martens, J. A.; Jacobs, P. A. Dealuminated H-Y Zeolites: Relation Between Physicochemical Properties and Catalytic Activity in Heptane and Decane Isomerization. *J. Phys. Chem.* **1996**, *100*, 12440.

(18) Gilson, J. P.; Edwards, G. C.; Peters, A. W.; Rajagopalan, K.; Wormsbecher, R. F.; Roberie, T. G.; Shatlock, M. P. Penta-Co-ordinated Aluminium in Zeolites and Aluminosilicates. *J. Chem. Soc., Chem. Commun.* **1987**, 91.

(19) Sanz, J.; Fornés, V.; Corma, A. Extraframework Aluminium in Steam- and $SiCl_4$-Dealuminated Y Zeolite. A ^{27}Al and ^{29}Si Nuclear Magnetic Resonance Study. *J. Chem. Soc., Faraday Trans.* **1988**, *84*, 3113.

(20) Chevreau, T.; Chambellan, A.; Lavalley, J. C.; Catherine, E.; Marzin, M.; Janin, A.; Hemedy, J. F.; Khabtou, S. Amorphization Levels, Nature and Localization of the Extraframework Phases of Dealuminated Y Zeolites. *Zeolites* **1990**, *10*, 226.

(21) Szostak, R. *Introduction to Zeolite Science and Practice*; Elsevier: Amsterdam, The Netherlands, 2001.

(22) Yang, R. T. *Adsorbents: Fundamentals and Applications*; John Wiley & Sons, Inc.: New York, 2003.

(23) Sanchez-Delgada, R. A. Breaking C-S Bonds with Transition Metal Complexes. A Review of Molecular Approaches to the Study of the Mechanisms of the Hydrodesulfurization Reaction. *J. Mol. Catal.* **1994**, *86*, 287.

(24) Mitchell, P. C. H.; Green, D. A.; Payen, E.; Tomkinson, J.; Parker, S. F. Interaction of Thiophene with a Molybdenum Disulfide Catalyst—An Inelastic Neutron Scattering Study. *Phys. Chem. Chem. Phys.* **1999**, *1*, 3357.

(25) Hughes, D. L.; Richards, R. L.; Shortman, C. A Series of μ-Disulphido-dimolybdenum (IV) Complexes: X-Ray Structure of the Novel (μ-Tetrahydrothiophene) Complex $[(C_4H_8S)Cl_3Mo(\mu\text{-}S_2)(\mu\text{-}C_4H_8S)MoCl_3(C_4H_8S)]$. *J. Chem. Soc., Chem. Commun.* **1986**, 1731.

(26) Gates, B. C.; Topsøe, H. Reactivities in Deep Catalytic Hydrodesulfurization: Challenges, Opportunities, and the Importance of 4-Methyldibenzothiophene and 4,6-Dimethyldibenzothiophene. *Polyhedron* **1997**, *16*, 3213.

(27) Ma, X.; Sakanishi, K.; Isoda, T.; Mochida, I. Quantum Chemical Calculation on the Desulfurization Reactivities of Heterocyclic Sulfur Compounds. *Energy Fuels* **1995**, *9*, 33.

(28) Janin, A.; Maache, M.; Lavalley, J. C.; Joly, J. F.; Raatz, F.; Szydlowski, N. FTIR Study of the Silanol Groups in Dealuminated HY Zeolites: Nature of the Extraframework Debris. *Zeolites* **1991**, *11*, 391.

(29) Chambellan, A.; Chevreau, T.; Khabtou, S.; Marzin, M.; Lavalley, J. C. Acidic Sites of Steamed HY Zeolites, Active for Benzene Self-Alkylation and Hydrogenation. *Zeolites* **1992**, *12*, 306.

(30) Miessner, H.; Kosslick, H.; Lohse, U.; Parlitz, B.; Tuan, V. A. Characterization of Highly Dealuminated Faujasite-Type Zeolites: Ultrastable Zeolite Y and ZSM-20. *J. Phys. Chem.* **1993**, *97*, 9741.

(31) Beran, S.; Jíru, P.; Wichterlová, B. Quantum-Chemical Study of the Physical Characteristics of Al^{3+}, $AlOH^{2+}$, and $Al(OH)_2^+$ Zeolites. *J. Phys. Chem.* **1981**, *85*, 1951.

(32) Beran, S. Quantum-Chemical Study of the Lewis Sites in Dehydroxylated Faujasite Zeolites. *J. Phys. Chem.* **1981**, *85*, 1956.

(33) Catana, G.; Baetens, D.; Mommaerts, T.; Schoonheydt, R. A.; Weckhuysen, B. M. Relating Structure and Chemical Composition with Lewis Acidity in Zeolites: A Spectroscopic Study with Probe Molecules. *J. Phys. Chem. B* **2001**, *105*, 4904.

(34) Parker, L. M.; Bibby, D. M.; Burns, G. R. Interaction of Water with the Zeolite HY, Studied by FTIR. *Zeolites* **1991**, *11*, 293.

(35) Kabe, T.; Ishihara, A.; Zhang, Q. Deep Desulfurization of Light Oil. 2. Hydrodesulfurization of Dibenzothiophene, 4-Methyldibenzothiophene and 4,6-Dimethyldibenzothiophene. *Appl. Catal., A* **1993**, *97*, L1—L9.

Received for review December 30, 2007
Revised manuscript received June 30, 2008
Accepted July 12, 2008

IE701785S